RESEARCH METHODS AND INNOVATIVE APPLICATIONS IN MATERIALS AND METALLURGY ENGINEERING

EDITOR
ASSOC. PROF. HAYRETTIN TOYLAN, PH.D.

9 786258 513424

DOI:10.5281/zenodo.18092955

Research Methods and Innovative Applications in Materials and Metallurgy Engineering

Editor

Assoc. Prof. Hayrettin Toylan, Ph.D.

Publisher
Platanus Publishing®

Editors in Chief
Assoc. Prof. Hayrettin Toylan, Ph.D.

Cover & Interior Design
Platanus Publishing®

The First Edition
December, 2025

ISBN
978-625-8513-42-4

Platanus Publishing®
Address: Natoyolu Cad. Fahri Korutürk Mah. 157/B, 06480, Mamak, Ankara, Turkey.

Phone: +90 312 390 1 118
web: www.platanuspublishing.com
e-mail: platanuskitap@gmail.com

Platanus Publishing®

CONTENTS

CHAPTER 1

An Unmanned Aerial Vehicle (UAV) Modelling and Simulation

Furkan Sarsılmaz[1] & Engin Can Girginel[2]

[1] Assoc. Prof. Dr., Fırat University, Faculty of Technology, Department of Mechatronic Eng., ORCID: 0000-0001-5351-8645
[2] Ph.D. Student at Bursa Technical University | M.Sc. Mechatronics Engineer, ORCID: 0000-0002-3387-7621

1. INTRODUCTION

Unmanned Aerial Vehicle (UAV); an aircraft that does not carry a pilot and/or passengers, can only carry certain equipment necessary for its function (such as digital equipment for image capture), is controlled by an operator in the flight area and/or can perform tasks that are difficult and dangerous for humans to perform using automatic flight methods included in its software. UAVs derive their lifting force from aerodynamic flight forces and powered propulsion units. In general, they can be classified into two categories based on their technical characteristics (weight, energy/fuel source, wing design, and the ability to be controlled remotely or autonomously) and their intended use: military (weapons, attack, reconnaissance) or non-military (commercial, hobby, scientific). According to the ICAO circular, unmanned aerial vehicles are mainly divided into two classes: remotely controlled or automatic (Mohsan S. et. all)

UAVs have been used for various purposes, such as attack, mapping, and reconnaissance, from the past to the present. When examining the early uses of UAVs, it is seen that they were first used during World War I. When examining the early history of UAVs (the first pilotless aircraft) (Ruston Proctor Aerial Target), it is concluded that they were developed through the work of A. M. Low (1916) using radio technology. The first unmanned use was also during World War I (September 12, 1917) with an automatic aircraft called "Hewitt-Sperry". When examining geomatics studies, Przybilla & Wester (1979) emphasize that their first experimental studies for photogrammetric purposes were the first civilian studies in the field of UAVs.

Numerous studies on UAVs continued not only during World War II but also after the war, and they have been used in many military operations and wars from the past to the present. In particular, the applications made after World War II were of great importance in terms of the development of missile models such as "Cruise," "Harpoon," and "Tomahawk." Looking at the recent past, it is observed that UAVs have evolved into devices that can perform their tasks by drawing their own routes using routing algorithms, in addition to being controlled remotely. Tulum, Durak, & İder (2009) conducted a routing algorithm study to enable unmanned aerial vehicles that detect threat areas and regional geography to plot routes between two points. Similarly, Lerma, Liu, Wang, Yi & Liu (2009) conducted a study using UAVs for close-range photogrammetry, emphasizing the maneuverability of cameras provided that the distance between the object to be photographed and the UAV is no more than 200 m.

Recently, the UAV market has developed rapidly, especially in the defense sector, becoming an integral part of our daily lives. In fact, the use of unmanned aerial vehicles has yielded very efficient results in some disputes, and studies in this area continue with increasing momentum. Unmanned aerial vehicles are currently used in civilian applications such as search and rescue operations,

mapping, intelligence-related work in the security sector, observation studies specific to a particular region, monitoring of coastal areas, firefighting, infrastructure observation, spraying of agricultural pesticides on crops, and aerial surveillance to locate or track criminals and suspect urban transformation observations in urbanization, three-dimensional modeling of cities, and observation and tracking in natural disasters. (Pan, et. all. 2022)

When reviewing international literature, unmanned aerial vehicles are referred to as "drones" or "UAS/UAV (Unmanned Aerial Vehicle/Systems)," but when certain technical characteristics are disregarded, they are seen to have the same meaning. Although they were initially known as drones, they are generally referred to as UAS/UAV/İHA in civilian use due to the perception formed in society for this reason, as well as their exposure to military or weapon-related uses, since they did not possess the technical capabilities they have today at that time. Considering this distinction, it is observed that automatically maneuverable sea or air vehicles are referred to as "drones," while aircraft equipped with engines, capable of flying without human intervention, controllable, and not carrying weapons such as "cruise missiles" are referred to as "UAVs." It has been determined that the definition expanded by the FAA encompasses small aircraft weighing less than 25 kg without a pilot and some components of these aircraft, and is used as the abbreviation "UAS (Unmanned Aircraft/Aerial Systems)" (Jin, et all 2005) Based on the definitions and explanations provided, the terms "UAS/UAV" and "drone" refer to the same concept. When examining the UAS/UAV concept, it corresponds to equivalent terms. Based on the definitions and explanations provided, the terms "UAS/UAV" and "drone" refer to the same concept. When examining the UAS/UAV concept, it is seen that it corresponds to equivalent terms and can be examined under two separate headings. The first heading can be expressed as the concept of Remotely Piloted Aircraft Systems/RPAS, where the operator coordinates remotely from the runway and controls the aircraft in this manner. This concept also includes equipment such as launch ramps, along with the connections that enable control. The second heading is "Autonomous (Automatic) UAS." At this stage, the operator does not intervene, and control is fully automated with the help of computerized control. In addition, "Automatic UAS" cannot be used in most countries due to restrictions arising from legislation and is not included in the definition of unmanned aerial vehicles. In conclusion, there are no clear boundaries between the terms "RPAS," "UAV/UAS," and "drone" in both international usage and usage by pilots (Meng, & Xin, 2010).

The materials used in UAV production must be particularly lightweight. For this purpose, lightweight metal materials are often preferred for their resistance to physical climatic conditions, toughness, high strength, and ability to prevent radio frequency interference. Lightweight metal materials are considered to be

metals with a specific gravity of less than five, such as aluminum, potassium, sodium, magnesium, and titanium.

One of the most important elements of UAVs is the body legs, which must be made of strong and non-flexible materials to ensure that they land firmly on the ground during landing. Fuselage profiles made of light metals or composite materials reduce the weight carried during flight, facilitating faster and more agile movements (Veyna, et all. (2021) and Santos, et all. (2018), The fact that the fuselage profile is made of durable material is also a factor that reduces damage to the UAV despite its exposure to outdoor weather conditions.

During flight, some minor deviations may occur in unmanned aerial vehicles due to environmental conditions. While there are various causes for these deviations, some of them are addressed by methods such as designing the wing structures in a square shape, using magnesium alloy lightweight metal materials, and increasing the use of composite materials due to their lightweight advantage (Schmidt, 2011).

This study simulates a quadrotor-type UAV model designed using SolidWorks software, featuring four rotors that operate independently of one another, as well as a drone that moves along a linear path created in a virtual environment using CoppeliaSim (V-Rep) simulation software and Lua language code. The current modeling and simulation will contribute positively to providing cost-effective, easy, and realistic control of unmanned aerial vehicles.

2. MATERIALS AND METHODS

2.1. Drone Modeling and Simulation with SolidWorks and CoppeliaSim (V-Rep) Simulator Programs

Unmanned Aerial Vehicles (UAVs), which are used in many military and civilian applications today, have become a highly relevant research topic for designers, simulation developers, and researchers. Thanks to modeling and simulation programs that are constantly advancing, technology development times have been reduced, and quality and efficiency have been improved day by day. In the design to be implemented in this study, a drone with four rotors was considered. The program to be used is SolidWorks, which was mentioned earlier. As can be understood from the way the four-rotor UAV concept is described, UAVs are named according to the number of rotors they have and their physical appearance. Among the different types, the most studied are those with four rotors. Therefore, it is observed that agile and aerodynamically efficient models are obtained in terms of design. The drone assembly designed in the SolidWorks (2019) program in this study is shown in Figure 1

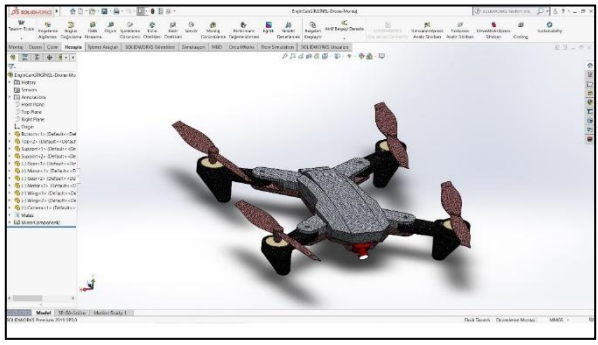

Figure 1. Drone designed for this study in SolidWorks (2019)

The planned quadcopter-type drone structure derives its lift force from rotating beams. For this reason, symmetrically placed propellers are planned to be used. This will ensure that all four propellers generate equal lift force, thereby equalizing the forces applied to the ground, enabling smooth takeoff, landing, flight, and hovering maneuvers. The efficiency loss often encountered in helicopters due to the tail motor will also be prevented by using four identical motor and propeller systems. With its integrated electronic control systems and electronic sensors, the design will resemble the "DJI 4730F" drone model in terms of its small size and successful maneuverability, making it suitable for both indoor and outdoor use. Unlike helicopters, there will be no need for mechanical connections to change the propeller angle. This will result in a simple design, reducing maintenance costs and efforts. Since four motors will be used, their diameters will be small, meaning that in the event of an accident, the motors will sustain less damage, and post-accident repair costs will be minimized as much as possible. Another result of this situation will be the ability to provide short-term flight due to the small size of the engines. The optimum operating speed will be selected by determining the amount of drag force at which speed and applying the iteration method. The validity of the predictions made during the optimization studies, the number of iterations, and the quality of the iterations are determinants of efficient optimization. It is expected that the air circulation will be increased thanks to the air gaps planned to be opened on the wings, and that this will contribute positively to engine performance by providing both aerodynamic structure and engine cooling support. In the chassis design, the landing gear's height from the ground, grip strength, arms designed to prevent vibration, absence of skew, slippage, excess, deficiency, or curvature in the axes, and a battery compartment of a size that allows the battery to be securely fixed in place are planned. The goal is to maintain aerodynamic flow in the area extending from the wing to the connection line, and drag is planned to be minimized as much as possible. This goal will be maintained at the end of the body, and for this reason, the body angle has been set below 30 degrees. Thanks to its double foldable wings, the drone is expected to be easily transportable.

The V-Rep scene environment for the drone-controlled security system developed in this study is shown in Figure 2, and an example of drone simulation movement is shown in Figure 3.

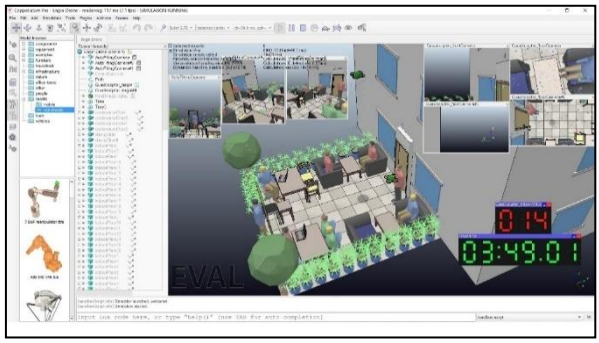

Figure 2. Drone-controlled security system developed in this study using the V-Rep Simulator

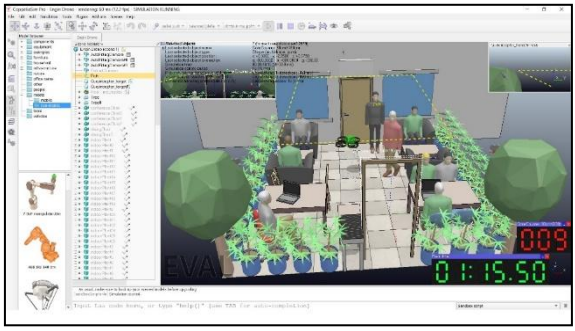

Figure 3. A drone changing direction by following the path specified in the V-Rep Simulator program.

The robot's simulation algorithm tests and mobility can be developed using the LUA language found in the V-REP program. The LUA language, which enables the coding of V-Rep simulations, is a software language released in 1993 that is similar to the C language and is defined as a programming language designed mainly for embedded systems and processors.

3. FINDINGS AND DISCUSSION

In today's living conditions, especially in densely populated metropolitan areas, controlling large groups of people is becoming increasingly difficult and is causing security vulnerabilities in countries. The current needs arising in areas such as shopping malls, cafes, and restaurants—where the likelihood of encountering risks posed by such crowds is high—along with factors like the inadequacy of human resources and the rapid growth of urban populations, necessitate the use of drone-based systems to control these areas (Dai, Ke, Quan,

& Cai, 2021). A drone structure that can successfully meet this societal need presents itself as both a technological and efficient solution, forming the basis of this thesis study. In this study, the CoppeliaSim (V-Rep) Simulator program was used to realistically experience the various details of this environment in daily life, while the Solidworks (2019) program was used for drone design studies.

3.1. Design Findings and Discussion of the Drone Project for Shopping Center Security

The modeling process used in different engineering applications on a sectoral basis is an important stage. The design and analysis stage, which forms the basis of the simulation stage, is carried out in many programs under today's conditions. The solid models created as a result of this step are important in terms of substantiating the physical work to be done. When some studies in the literature are examined, certain advantages such as widespread use, efficiency, and ease of use are shared or common to the SolidWorks (2019) program, which was preferred in this study. The drone parts designed for this study are shown in Figures 4 and 5

Figure 4. An example of a drone assembly and its parts, which is the subject of this study, designed using SolidWorks (2019) software.

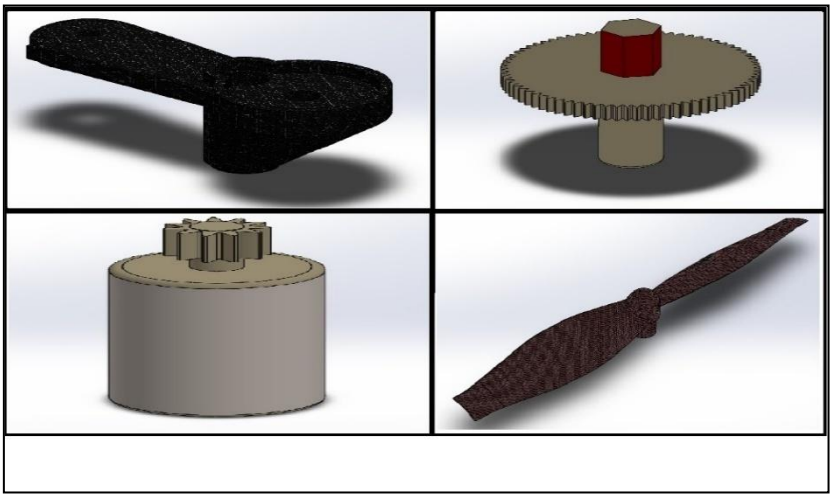

Figure 5. Parts belonging to the drone assembly that is the subject of this study, designed using SolidWorks (2019) software.

3.2. Findings and Discussion of the CoppeliaSim (V-Rep) Simulation of the Drone Project for Shopping Center Security

Developed as a general-purpose robot simulation, the "Virtual Robot Experimental Platform" simulation program, a product of "Coppelia Robotics," is now known as CoppeliaSim. Its customized user interface, modular structure that integrates a development environment with a high degree of realism, the ability to use various objects under different conditions, the ease of use of the simulation environment, rapid prototyping, the usability of the prototyped product, the simplicity of the algorithm designs in the projects, and the ability to simulate three-dimensional real-world environments with high detail during active simulation.

When reviewing the literature, it is observed that the various simulation programs used in the studies either stand out or remain in the background due to their different features. The program selected for use in this thesis study, which simulates the experimental possibilities of a shopping mall café design and whose findings will be detailed and discussed, will be described in this section along with the experimental environment created within the program.

In this project, security control is provided by two drones, one of which moves along a predetermined route using distance sensors to avoid colliding with any objects, while simultaneously capturing real-time images using the security camera mounted on it to ensure the safety of the environment. The camera data obtained is displayed on the security officer's laptop screen via a desktop application and stored in the recording archive for a specified period.

In this study, due to the simulation environment, camera images are displayed and recorded in real-time within the simulation environment. The possibility that

the camera angle of the drone moving along a specific running route may be insufficient in certain situations could lead to potential security vulnerabilities. To prevent this, another drone is used to capture images in real time thanks to its camera, which is fixed at a higher altitude and has a relatively wider angle. To increase the visibility of possible blind spots, fixed cameras are placed inside two trees located at the corners of the cafe. In this way, security checks are carried out using both drone camera footage and fixed camera footage, blind spots are eliminated, and the number of people entering and leaving the cafe daily is counted using a counter placed at the X-ray machine at the entrance, with one person added for each individual seen. This number enables both the detection of daily crowd density in the café and the identification of whether a particular individual is suspicious, by matching the corresponding number with the camera time. The simulation scene findings mentioned and obtained are shown in Figure 6, which depicts the drone simulation and security control system scene screen designed in the CoppeliaSim (V-Rep) program, Figure 7 shows images from drones capable of running along a specific route and drones with fixed movement, Figure 8 shows images from a camera fixed on trees and a camera fixed on a door on a wall, along with simulation parameters. Figure 9 illustrates the real-time object used, a counter object measuring 80cm x 190cm, and the control units for the simulation's speed and motor parameters.

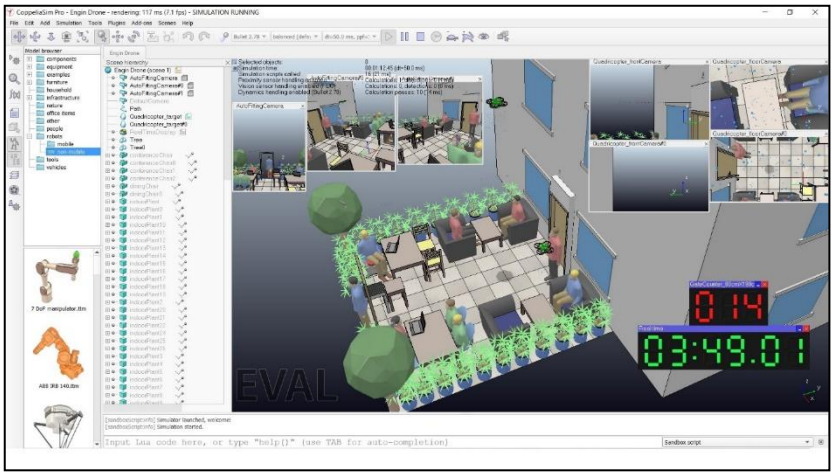

Figure 6. Simulation screen of the scene designed on the CoppeliaSim (V-Rep) program in this study.

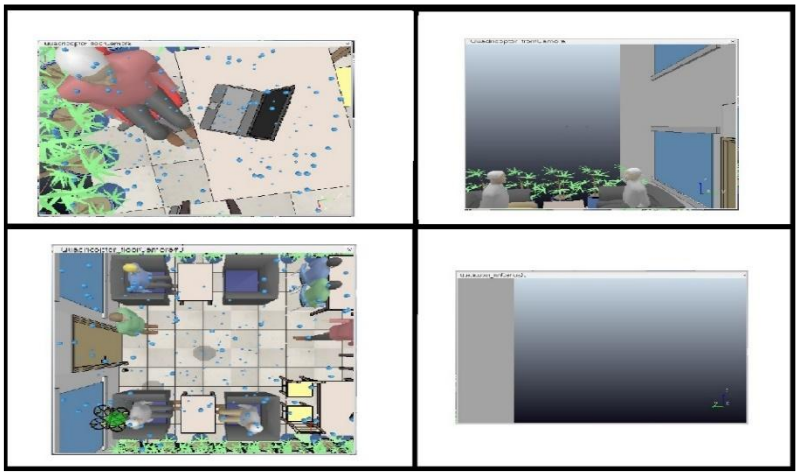

Figure 7. Images from drones capable of flying along a specific route and drones capable of stationary movement.

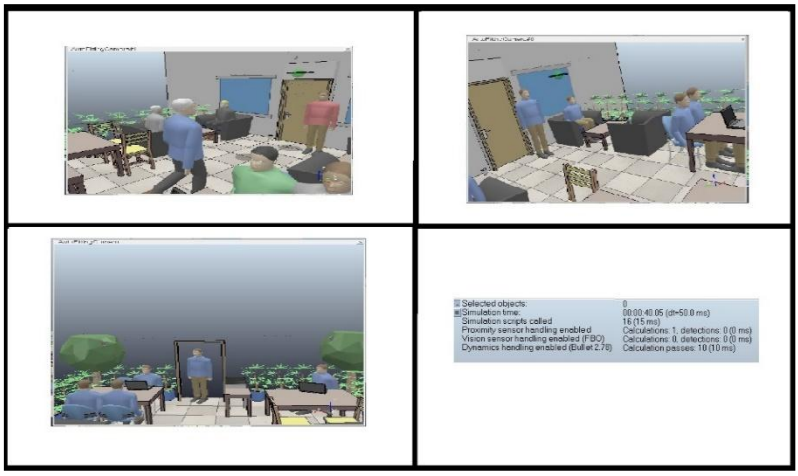

Figure 8. Images from cameras mounted on trees and on a door in the wall, and simulation parameters

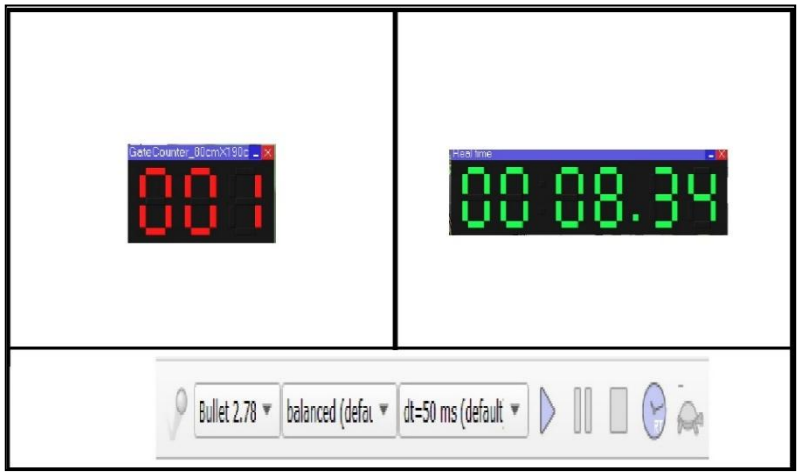

Figure 9. The real-time object used, the counter object measuring 80 cm x 190 cm, and the control units for the speed and motor parameters of the simulation belonging to the scene.

The experiment codes are written in Lua language. A drone structure that can move under Lua language control with line tracking control is used in the simulation scene.

It has data types such as nil (zero), Boolean (logical operation), number, string, and tables. “And”, “break”, “do”, “else”, “elseif”, “end,” “false,” “for,” “function,” “if,” “in,” “local,” “nil,” “not,” “or,” “repeat,” “return,” “then,” “true,” “until,” and “while” keywords. The “+” operator is used to perform addition between two or more variables, the “-” operator is used for subtraction, the “*” operator is used for multiplication, the “/” operator is used for division, the “%” operator is used for percentage, and the “^” operator is used for exponentiation. Just like in the C programming language, comparison operators are also available in the LUA language. The comparison operators mentioned are “==,” “~=,” “>,” “<,” “>=,” and “<=.” There are also logical operators in the LUA language. These are called the “and,” “or,” and “not” operators. The mathematical operators in the language can generally be divided into five different groups. These are trigonometric operators (“math”, ‘acos’, “math.asin”, “math.atan”, “math.atan2”, “math.cos”, “math.rad”, “math.deg”, “math.pi”, “math.sin”, “math.tan”), functions ("math. abs,“ ”math.log,“ ”math.sqrt,“ ”math.exp“), maximum/minimum operators (”math.max,“ ”math.min“), rounding/remainder operators (”math. ceil,“ ”math.floor,“ ”math.fmod,“ ”math.modf“), and random operators (”math.random,“ ”math.randomseed,“ ”os.time"). The value entered into the desired mathematical function is returned as the answer. For example, the function written as math.sqrt(x) returns the x value specified in parentheses. A string value to be printed to the screen is printed

using the “print” command. The code for the situation described is written as shown in example 1. Here, the text “Muhendis Engin” will be printed to the console screen. Example 2 describes the operations that add the two numerical values “c” and “d” and ‘say1’ and “say2” together.

Example 1: (1)

```
name=‘Engin’
print=(‘Muhendis ’ . . name)
```

Example 2: (2)

Operation1:

```
function sum(c,d)
return c+d
end
```

Operation2: (3)

```
say1=4
say2=5
result=sum(say1,say2)
print(result)
```

The code algorithms mentioned are written in the script areas belonging to the objects. The target child script-threaded code that controls the target of the drone object moving along a specific path is shown in Figure 10, and the child script codes that provide control of this drone object are shown in Figures 11 and 12, respectively.

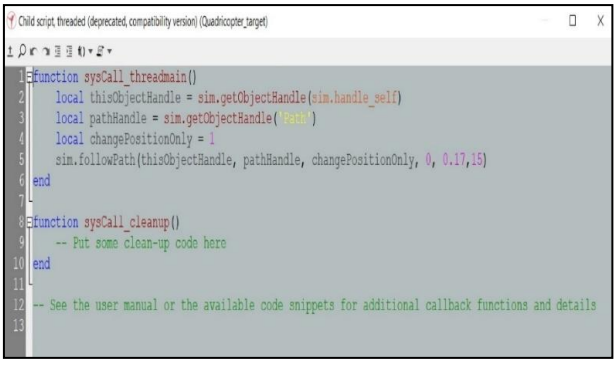

Figure 10. Target child script-threaded code controlling the target of a drone object moving along a specific route

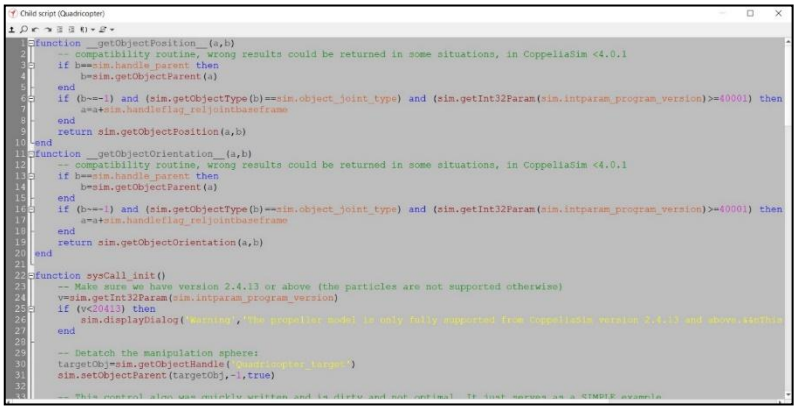

Figure 11. Child script codes that control a drone object moving along a specific route

Figure 12. Child script codes that control a drone object moving along a specific route

4. Conclusion

The following conclusions were reached in the general evaluation of the modeling and simulation of unmanned aerial vehicles.

1) CoppeliaSim (V-Rep) program was examined in detail, and its high effectiveness was observed, especially in simulation and modeling. The program can perform effective operations by handling multiple data inputs with mathematical calculations. This led us to conclude that, as applied in this study, the movement pattern defined by a specific route drawn on a modeled or pre-existing drone object in the program and program codes written in Lua language can contribute positively to our lives by creating a drone-controlled security system.

2) In the studies conducted, it was observed that drones, as aerial vehicles, are classified into different types based on their characteristics such as wing structure, power, number of wings, and number of motors. Among these types, the quadcopter structure has four arms and four rotors, the hexacopter structure has six motors and three supports, the octocopter structure has eight motors and four support arms, and the tricopter structure has three propellers, three motors, and mostly three supports, which has been the reason for its preference. The reasons for this preference include: the symmetrical placement of four propellers, each producing equal lift force, ensuring that the forces applied to the ground are equal, enabling smooth takeoff, landing, flight, and hovering maneuvers, and allowing for a design that can be flown in shopping mall conditions due to its small size and successful maneuverability. the use of four motors results in smaller motor diameters, reducing potential damage in the event of an accident, a simple design, and reduced maintenance costs, post-accident repair costs, and effort.

3) The materials used in the drone structure were examined in detail, and it was observed that aluminum material is more advantageous than carbon fiber or wood material in the event of a fall, as predicted by the observed results. In addition, it was determined that aluminum is more expensive than wood material and heavier than carbon fiber material. In particular, it was observed that propellers made of carbon fiber, wood, and fiberglass are the best performing materials for unmanned aerial vehicles, while plastic propellers are inexpensive, flexible, and cause vibration and, as a result, power loss. As a result of these observations and findings, carbon fiber propellers were selected for the drone design, particularly due to their performance advantages, and a design was created in SolidWorks based on this material selection.

4) In this master's thesis study, a quadcopter with a successful design was created, in which the mechanical structure of the frame was designed using lightweight materials such as aluminum alloy and carbon fiber to be able to carry both its own weight and the weight of the equipment mounted on it that is suitable for the task at hand, It was concluded that the quadcopter should have sufficient motor and propeller power to meet the requirements, with mechanical, aerodynamic, and lift force elements taken into consideration, and that a well-designed controller structure should be supported by the correct element selection.

Acknowledgements

This paper is derived from the author's (ORCID: 0000-0002-3387-7621) master thesis entitled "***Drone Modelling and Simulation*** " and the publicated with 782330 thesis number.

References

Mohsan, S. A. H., Khan, M. A., Noor, F., Ullah, I., & Alsharif, M. H. (2022). Towards the unmanned aerial vehicles (UAVs): A comprehensive review. *Drones*, vol.6,(6), pp.147. https://doi.org/10.3390/drones6060147

Przybilla, H.-J. & Wester, E. W. (1979). Bildflug mit ferngelenktem Kleinflugzeug, In: Bildmessung und Luftbildwesen, Zeitschrift fuer *Photogrammetrie und Fernerkudung*, vol. 47, (5), pp.137-142.

Tulum, K., Durak, U. & Yder, S. (2009). Situation aware UAV mission route planning. *2009 IEEE Aerospace Conference,* Big Sky, Montana, USA, 112.

Lerma, F. A., Liu B., Wang Z., Yi B.& Liu,S (2009). Role of image-guided patient repositioning and online planning in localized prostate cancer IMRT, *Radiotherapy and Oncology*, vol. 93 (1), pp.18-24.

Pan, Z., Zhang, C., Xia, Y., Xiong, H., & Shao, X. (2022). An improved artificial potential field method for path planning and formation control of the multi-UAV systems. *IEEE Transactions on Circuits and Systems II: Express Briefs*, vol.69 (3), pp.1129–1133. https://doi. org/10.1109/TCSII.2021.3112787

Jin, Y., Liao, Y., Minai, A. & Polycarpou, M. (2005). Balancing Search And Target Response in Cooperative Unmanned Aerial Vehicle (UAV) Teams. *IEEE Transactions on Systems, Man, and Cybernetics-Part B:* Cybernetics, vol 36, (3), pp.571-587.

Meng, H.& Xin, G. (2010). UAV Route Planning Based on the Genetic Simulated Annealing Algorithm. *International Conference on Mechatronics and Automation (ICMA)*, 4-7 Agust, Xi'an, pp. 788-793.

Schmidt, M. D., Simulation and Control of A Quadrotor Aerial Vehicle, M.Sc. Thesis, University of Kentucky, (2011). https://uknowledge.uky.edu/g radschool_theses/93/

Veyna, U., Garcia-Nieto, S., Simarro, R., & Salcedo, J. V. (2021). Quadcopters testing platform for educational environments. *Sensors*, vol 21, (12), pp. 4134. https://doi.org/ 10.3390/s21124134.

Santos, M. F., Silva, M. F., Vidal, V. F., Hon´ orio, L. M., Lopes, V. L. M., Silva, L. A. Z., Rezende, H. B., Ribeiro, J. M S., Cerqueira, A. S., Pancoti, A. A. N., & Regina, B. A. (2018). Experimental validation of quadrotors angular stability in a gyroscopic test bench. *2018 22nd International Conference on System Theory*, *Control and Computing,* Sinaia, Romania. https://doi.org/10.1109/ICSTCC.2018.8540660.

Dai, X., Ke, C., Quan, Q., & Cai, K. (2021). RFlySim: Automatic test platform for UAV autopilot systems with FPGA-based hardware-in-the-loop simulations.

Aerospace Science and Technology, vol.114, Article 106727. https://doi.org/10.1016/j. ast.2021.106727

CHAPTER 2

Evaluation of Iron Ore Tailings as a Strategic Precursor in Geopolymer Systems

Kemal Şahbudak[1]

[1] Doç. Dr., Sivas Cumhuriyet Üniversitesi, Metalürji ve Malzeme Mühendisliği Bölümü, 000-0003-4853-6843

1. Introduction

Iron and steel production remains one of the fundamental pillars of modern infrastructure systems, industrialization, and global economic development, while simultaneously generating significant environmental burdens. The global increase in this production has led to the generation of large quantities of iron ore tailings (IOT) during ore beneficiation processes. The literature reports that, on average, 0.4–0.6 tons of IOT are produced per 1 ton of processed iron ore, and in some mining operations this amount can reach 1–2 tons. These high generation rates have made IOT one of the largest industrial solid-waste streams worldwide (Zhang et al., 2021; Almeida et al., 2023).

The accumulation of iron ore tailings mainly in tailings dams or open storage areas entails multidimensional environmental risks, including land occupation, dam stability problems, dust emissions, heavy-metal leakage, contamination of groundwater and surface water, and ecosystem degradation. Despite high capital and operating costs, current storage practices cannot fully eliminate these risks in the long term; in particular, dam failures and chronic environmental impacts have turned IOT management into one of the most critical challenges in the mining sector. This situation necessitates rethinking iron ore tailings not merely as waste requiring disposal, but as a strategic secondary raw material resource.

On the other hand, the climate crisis, carbon-neutral targets, and resource-efficiency policies have led to intensified scrutiny of conventional Portland cement due to its high energy consumption and CO_2 emissions. In this context, geopolymers and, more broadly, alkali-activated binder systems stand out among sustainable construction materials thanks to advantages such as a low carbon footprint, high mechanical performance, and the ability to valorize waste-based feedstocks. Aluminosilicate-rich fly ash, blast furnace slag, metakaolin, and various mine residues are among the commonly used raw materials in the development of these binder systems (Davidovits, 1991; Provis, 2018).

Iron ore tailings, characterized by high SiO_2, Al_2O_3, and Fe_2O_3 contents and a fine particle size distribution, have attracted attention as a promising feedstock for geopolymer and alkali-activated binder systems. However, the reactivity of IOT can vary significantly depending on its source, mineralogical composition, particle size, and applied pre-treatment methods, which directly influence the geopolymerization mechanism and final binder performance. Therefore, effective utilization of IOT in geopolymer production requires a holistic approach integrating environmental impact mitigation, material reactivity enhancement, and binder performance optimization.

1.1. Global Generation and Accumulation of Iron Ore Tailings

The rapid growth in global demand for iron and steel has led, in recent years, to critically high volumes of iron ore tailings (IOT) generated during ore

beneficiation processes. During iron ore processing, approximately 30–60% of the ore mass is converted into fine-grained waste, corresponding to an average production of 0.4–0.6 tons of IOT per ton of processed ore (Almeida et al., 2023). In certain regions, this ratio is even higher; for instance, in Western Australia, it has been reported that approximately 2 tons of IOT are generated for every 1 ton of iron ore produced (Kuranchie et al., 2016).

Waste generation associated with mining activities has increased markedly over the past century. Between 1915 and 2019, global mine waste production followed a continuously increasing trend, indicating that the rising rate of IOT generation has evolved from a regional concern into a global environmental challenge (Figure 1; Hamada et al., 2025).

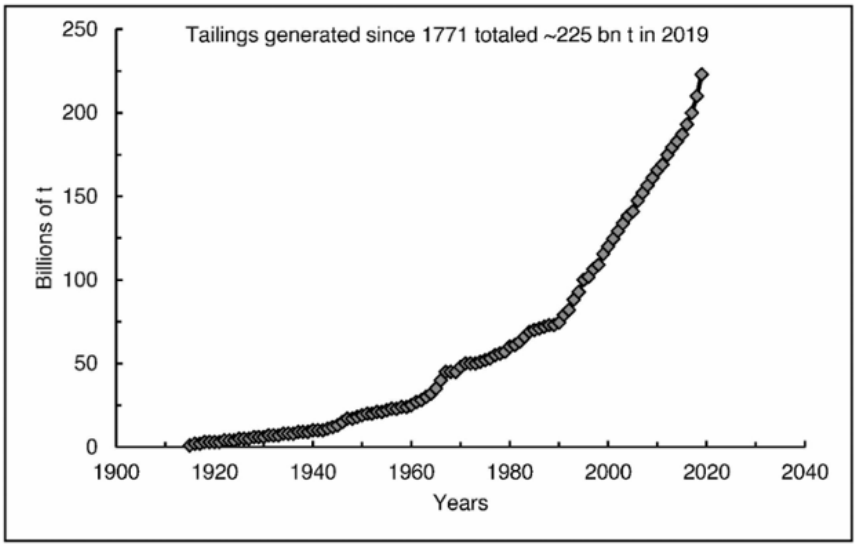

Figure 1. Global mine waste production (1915–2019)

High production rates have resulted in the accumulation of enormous quantities of waste worldwide. In China, the stockpiled volume of iron ore tailings has reached approximately 5–6 billion tons, with an additional 0.3–0.6 billion tons of new IOT generated annually (Huang et al., 2024; Zhao et al., 2026). At the global scale, annual IOT generation is estimated to be around 1.4 billion tons (Saldanha et al., 2023). In Brazil, annual IOT production is approximately 154 million tons, while the accumulated stock has reached nearly 4 billion tons (Ramos et al., 2024). Collectively, these figures clearly demonstrate that IOT constitutes one of the largest industrial solid waste streams worldwide.

Despite the substantial volumes generated, the reuse rate of iron ore tailings remains relatively low. In China, the comprehensive utilization rate was reported to be only 20–30% as of 2018 (Zhao et al., 2021a). The large quantities that cannot be reused are stored in tailings dams, resulting in both significant land occupation and rapidly increasing operational and safety-related costs. In this

context, the global expenditure required for the safe management of iron ore tailings dams is projected to exceed USD 2.2 billion (Zhao et al., 2026).

Large-scale storage of IOT gives rise to multiple challenges, including dust emissions, groundwater contamination, land degradation, and long-term environmental risks (Zhang et al., 2021). Consequently, the valorization of iron ore tailings as secondary raw materials—particularly in applications such as construction, cement, and geopolymer production—has emerged as a strategic necessity within the frameworks of the circular economy and low-carbon material technologies (Adiansyah et al., 2015; da Silva et al., 2022).

1.2 Environmental Risks and Impact Mechanisms of Iron Ore Tailings

Iron ore tailings (IOT) generated as a result of iron ore beneficiation activities pose significant environmental risks worldwide due to their large production volumes and fine-grained nature. During beneficiation, approximately 20–40% of the total ore mass is converted into IOT, making this material one of the largest solid waste components of mining operations (Saldanha et al., 2023). In countries with intensive mining activities, such as China and Brazil, the accumulation of IOT stocks reaching billions of tons represents a critical challenge in terms of the long-term stability of tailings dams, extensive land occupation, and increasing pressure on surrounding ecosystems (Ramos et al., 2024).

The environmental impacts associated with IOT are widely analyzed within the framework of multilayered pollution processes arising from interactions between mine wastes and water, soil, and air compartments. Mechanisms such as heavy metal mobilization, acid mine drainage, dust dispersion, and ecosystem degradation indicate that these wastes are not merely physical pollutants, but rather dynamic systems capable of inducing persistent and long-term environmental effects through complex biogeochemical processes. The interactions between these mechanisms and environmental components are schematically summarized in Figure 2 (Tharwat et al., 2023; Zhang et al., 2021).

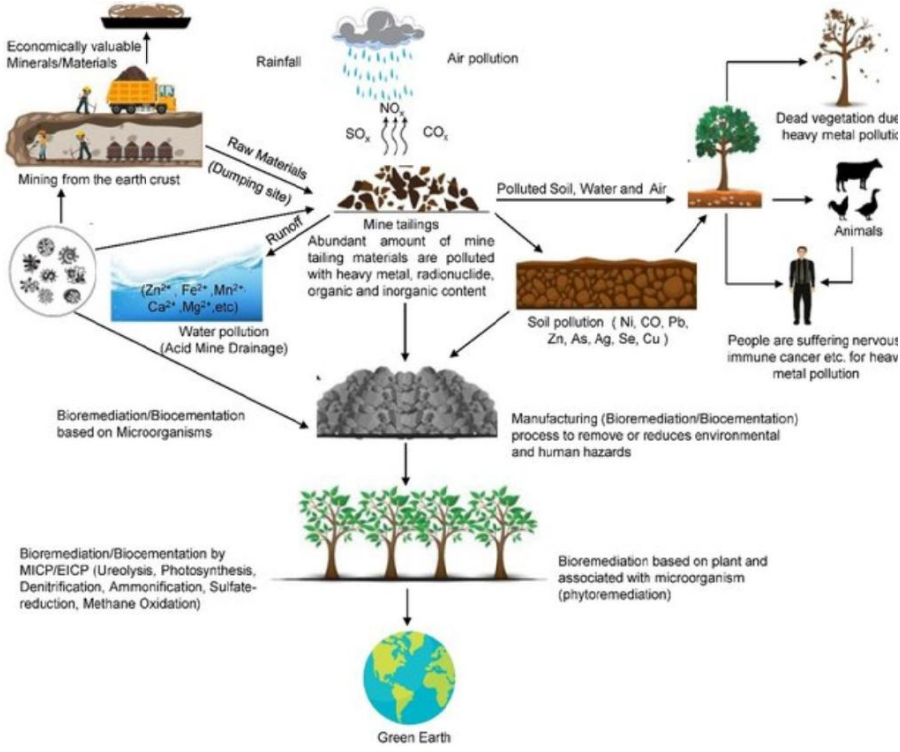

Figure 2. Impacts of mine tailings and biological remediation approaches (Tharwat et al., 2023)

The environmental impacts of IOT also pose substantial risks to human health due to the presence of potentially toxic elements. Deterioration of structural stability on tailings dam surfaces and dry storage areas enhances dust generation under wind action; exposure to heavy metals through fine particulates may result in persistent adverse effects, particularly affecting the respiratory system (Soltani et al., 2021; Makarov et al., 2021). In addition, the microstructural characteristics of construction materials incorporating IOT play a decisive role in water permeability and potential contaminant release, rendering such materials sensitive to environmental conditions (Zhang et al., 2021).

Over the long term, IOT accumulated on-site can facilitate the transport of heavy metals into soils and groundwater systems through rainfall infiltration and surface runoff. Particularly following dam failures or flooding events, markedly elevated heavy metal concentrations have been reported in riverbeds and floodplains, exerting severe pressure on ecosystem integrity and drinking water resources (Davila et al., 2020; da Silva et al., 2022). Moreover, the utilization of natural ecosystems as waste disposal sites due to insufficient storage capacity exacerbates forest degradation, soil erosion, and landslide risks (Castro-Gomes et al., 2012; Thejas & Hossiney, 2021).

The structural safety of IOT dams represents one of the most critical components of environmental risk management. Geotechnical vulnerabilities and operational deficiencies associated with upstream-type dams account for a significant proportion of the most catastrophic environmental disasters in the mining sector (Kossoff et al., 2014; Armstrong et al., 2019). In Brazil, the Samarco (2015) and Brumadinho (2019) dam failures released millions of cubic meters of tailings into the environment, causing long-term ecological degradation across extensive river basins (Silva Rotta et al., 2020). Reports of similar incidents in China and Mexico further confirm that the risks associated with IOT storage constitute a globally shared challenge (Cui et al., 2019).

When iron ore tailings are considered alongside other large-volume industrial wastes—such as coal fly ash (CFA) and municipal solid waste incineration fly ash (MSWI FA)—the cumulative environmental burden becomes even more pronounced. The limited reuse rates and long-term storage requirements of these wastes indicate that prevailing disposal-oriented management approaches are inherently unsustainable (Gollakota et al., 2019; Zhan et al., 2022). Given the approximately 1.4 billion tons of IOT generated annually worldwide, it is evident that management strategies relying solely on storage are not viable in the long term (Saldanha et al., 2023).

Conventional disposal methods, including metal recovery and classical site rehabilitation, suffer from significant limitations related to high energy demand, risks of groundwater contamination, and the need for prolonged post-closure monitoring (Sun et al., 2020). Consequently, IOT and similar industrial wastes should be regarded not only as environmental liabilities, but also as potential secondary raw material sources for geopolymer binders and other construction materials. The literature demonstrates that geopolymeric and ceramsite-based products derived from iron ore tailings can effectively mitigate environmental risks while delivering adequate mechanical and durability performance when appropriate mix designs and alkali-activation parameters are employed (Lu et al., 2020; Wang et al., 2020).

1.3. Low-Carbon Alternative Binder Systems: Geopolymers and Waste-Based Feedstocks

In the context of the growing emphasis on climate change mitigation and resource efficiency, geopolymers have increasingly attracted attention as a low-carbon and high-performance alternative to Portland cement. These binders are formed through polycondensation reactions of aluminosilicate-rich raw materials under highly alkaline conditions, resulting in a three-dimensional inorganic network structure. Owing to their broad raw-material flexibility and relatively low energy requirements, geopolymers offer significant environmental advantages (Davidovits, 1991; Provis & van Deventer, 2014). The literature indicates that geopolymer production can achieve 40–80% lower CO_2 emissions

compared with Portland cement, while simultaneously providing engineering-critical properties such as high compressive strength, low shrinkage, high-temperature resistance, and superior durability against chemical attack (Duxson et al., 2007; Deb et al., 2014).

One of the key drivers behind the growing adoption of geopolymer binders is the effective valorization of large volumes of industrial by-products and mine wastes. Fly ash–, blast furnace slag–, and metakaolin-based geopolymer systems have been demonstrated to deliver mechanical strength and durability comparable to—or exceeding—those of conventional cement-based systems when appropriate activator types and dosages are employed, at both early and long-term curing stages (Andini et al., 2008; Nematollahi & Sanjayan, 2014). In parallel, glass polishing waste, ceramic residues, and other industrial by-products have been successfully incorporated into geopolymer matrices, showing that this approach not only improves waste management practices but also reinforces circular economy principles (De Azevedo et al., 2021; Marvila et al., 2021).

In recent years, a marked increase has been observed in academic studies investigating mine tailings and industrial by-products either as supplementary cementitious materials (SCMs) or as direct binder constituents (Chandran et al., 2026). This trend clearly reflects and reinforces the global research direction toward the development of low-carbon binders, as well as the growing scientific interest in waste-based material technologies (Figure 3).

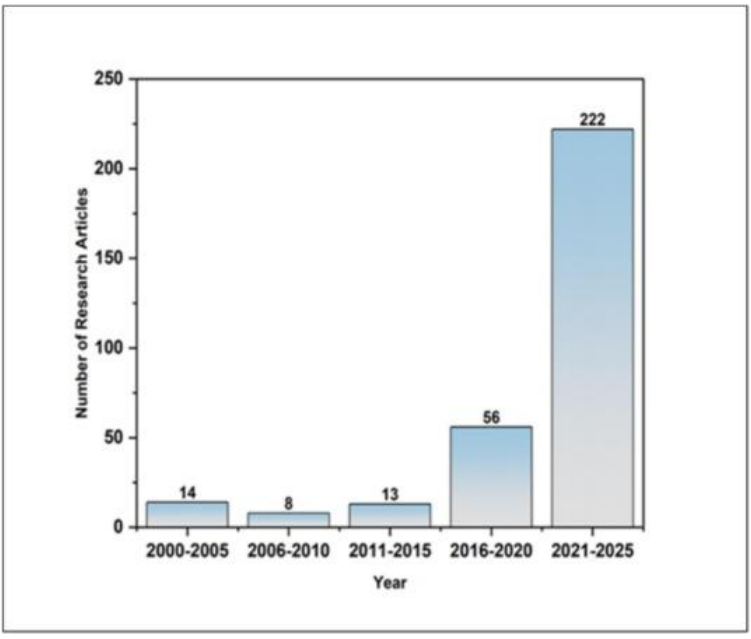

Figure 3. Annual growth of SCM-related research on mine tailings (2000–2025) (Chandran et al., 2026)

Geopolymers are regarded not only as environmentally friendly binders, but also as a “waste-sink” technology capable of linking different industrial sectors. Among the large-volume wastes generated by the mining industry, iron ore tailings (IOT) are of particular significance. Accounting for approximately 20–40% of the total ore mass, IOT has historically been stockpiled primarily in tailings dams and treated as an environmental burden. However, recent studies demonstrate that IOT can be utilized as a supplementary cementitious material (SCM) as well as fine and coarse aggregate in cementitious systems, thereby offering substantial potential as a raw material for alternative binder technologies (Kuranchie et al., 2016; Han et al., 2017).

Mortars and bricks produced by incorporating IOT into fly ash– and slag-based geopolymer systems have been reported to maintain—or, at certain replacement levels, even enhance—mechanical strength, while also yielding favorable outcomes in terms of porosity, water absorption, and microstructural continuity (Kumar et al., 2017; Ferreira et al., 2022). These findings indicate that IOT should not be regarded merely as a passive filler, but rather as a functional component capable of supporting binder performance under appropriate design conditions.

Research on the use of IOT in geopolymer systems extends beyond aggregate or passive filler applications. Mechanical and/or chemical activation treatments have been shown to impart pozzolanic characteristics to IOT, enabling its active participation in binder phase formation (Duan et al., 2016a; Yao et al., 2020). Mechanical activation enhances reactivity by increasing specific surface area and amorphous phase content, whereas chemical activation—via silica- or sodium silicate–based compounds—promotes the formation of additional binding phases within the geopolymer matrix (Saedi et al., 2020; Huang et al., 2024). In this context, studies demonstrating that sodium silicate derived directly from IOT can be used as an activator in one-part geopolymer systems highlight the potential for iron ore tailings to acquire direct chemical value (Figueiredo et al., 2021).

Another important trend supporting the advancement of geopolymer binders is the contribution of other large-volume wastes, such as coal fly ash (CFA) and municipal solid waste incineration fly ash (MSWI FA). Owing to its high amorphous glass content, CFA accelerates gel formation and promotes strength development in geopolymer matrices. MSWI FA, when subjected to appropriate pre-treatment and alkali-activation strategies, can contribute to heavy metal immobilization and the formation of durable binding phases (Gollakota et al., 2019; Zhan et al., 2022).

Collectively, these findings demonstrate that geopolymer binders are not merely laboratory-scale alternatives, but rather strong candidates for high-performance applications. In particular, the high cement consumption and associated CO_2 emissions of ultra-high-performance concrete (UHPC) render

geopolymer-based systems especially attractive from a sustainability perspective. The use of geopolymer binders produced through the alkali activation of industrial by-products—such as fly ash, slag, and IOT—in UHPC designs offers substantial potential for reducing carbon footprints while simultaneously converting wastes into high value-added products (Du et al., 2021; Huang et al., 2024).

A major step toward the practical implementation of geopolymer technology is the development of one-part geopolymer systems. Whereas the corrosiveness and handling challenges associated with liquid alkaline activators constrain industrial deployment of conventional two-part systems, one-part systems—comprising dry-mixed reactive components activated solely by water addition—offer cement-like workability and safer operating conditions (Luukkonen et al., 2018; Panda et al., 2019). The incorporation of IOT and other mine tailings into such systems represents a promising pathway for simplifying production processes and integrating large volumes of mining waste into the construction materials value chain (Ferreira et al., 2022).

1.4 Geopolymerization Potential and Activation Strategies of Iron Ore Tailings

Iron ore beneficiation residues (iron ore tailings, IOT) represent a highly promising precursor for geopolymer and, more broadly, alkali-activated binder systems, owing to both their abundance and chemical composition. The conversion of approximately 20–40% of the total ore mass into IOT during mining operations has rendered this material one of the largest solid waste streams worldwide. Annual generation reaching hundreds of millions of tons in Western Australia, combined with accumulated stocks in China approaching tens of billions of tons and sustained annual emissions on the order of hundreds of millions of tons, clearly demonstrates that reliance on storage-based management strategies is both economically and environmentally unsustainable (Han et al., 2017; Kuranchie et al., 2015; Almeida et al., 2023; Jiang et al., 2022; Zhao et al., 2021).

The construction, maintenance, and rehabilitation of tailings dams impose multi-billion-dollar costs globally, yet risks such as groundwater contamination, dust emissions, land degradation, and heavy metal leakage cannot be fully eliminated (Adiansyah et al., 2015; Adiguzel et al., 2022; da Silva et al., 2022; Davila et al., 2020; Schoenberger, 2016; Cui et al., 2021; Li Y. et al., 2023). Consequently, the transformation of IOT from a waste requiring disposal into value-added binder systems within a circular economy framework has become a strategic necessity (Lebre et al., 2017; Brown & Milke, 2016).

From a geopolymerization perspective, the chemical composition and mineralogy of IOT are particularly favorable for such a transformation. Typical IOT compositions reported in the literature contain approximately 20–70 wt.%

SiO_2, 6–70 wt.% Fe_2O_3, and varying amounts of Al_2O_3, CaO, and MgO. These oxides collectively provide the essential Si–Al framework and auxiliary flux phases required for geopolymer precursors (Li C. et al., 2009; Zhang Z. et al., 2016; Zhang N. et al., 2021; Carvalho et al., 2021; Almeida et al., 2021). Composed primarily of quartz, hematite, goethite, and clay minerals (e.g., kaolinite), IOT exhibits an aluminosilicate character comparable to that of widely used geopolymer raw materials such as fly ash and metakaolin. As noted by Yellishetty et al. (2008), its mineralogical framework closely resembles that of natural sands.

The fine particle size and high specific surface area of IOT promote silica–alumina polycondensation reactions under alkaline activation, enabling the formation of a denser and more continuous geopolymer network. This effect is particularly pronounced in superfine fractions, where reactivity is significantly enhanced (Ferreira et al., 2022; Wang et al., 2023; Yao et al., 2020). Moreover, the presence of Fe_2O_3 allows iron to partially adopt tetrahedral coordination during geopolymerization and to be incorporated into Si–O–T (T = Si, Al, Fe) linkages, thereby contributing to the formation of Fe–A–S–H–type networks. This behavior supports the development of hybrid gel systems in addition to conventional N–A–S–H and C–(A)–S–H gels (Kaze et al., 2017; Zhan et al., 2018).

The positions of different binder precursors within the CaO–SiO_2–(Al_2O_3+Fe_2O_3) compositional system and their dominant reaction mechanisms are schematically illustrated in Figure 4, highlighting the hybrid reaction potential of IOT within alkali-activated and geopolymer binder systems.

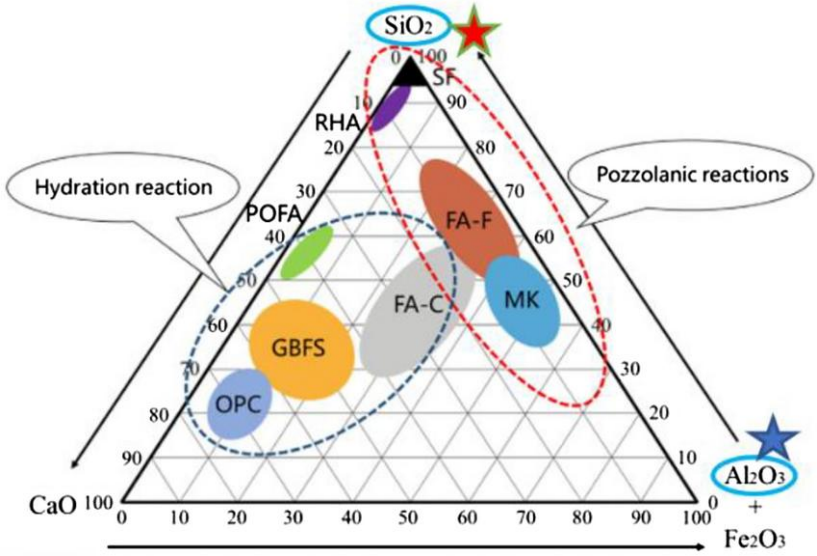

Figure 4. Position of binder precursors in the CaO–SiO_2–Al_2O_3/Fe_2O_3 system (Scrivener et al., 2018)

The $CaO–SiO_2–(Al_2O_3+Fe_2O_3)$ ternary diagram presented in Figure 4 illustrates the reaction mechanisms favored by different binder precursors (Hosseini et al., 2019). Materials with high CaO content—such as ordinary Portland cement (OPC) and ground granulated blast-furnace slag (GBFS)—are positioned within the hydration region, whereas aluminosilicate-rich precursors, including low-calcium fly ash (FA-F) and metakaolin (MK), fall within the pozzolanic/geopolymer reaction domain. The oxide composition of IOT reported in the literature—dominated by SiO_2, Al_2O_3, and Fe_2O_3—lies between these end-member behaviors, conferring a hybrid reaction potential that supports both N–A–S–H gel formation and, under suitable conditions, the development of calcium-bearing C–A–S–H gels. Accordingly, IOT is not only amenable to geopolymerization but also represents a strategic precursor for dual-mechanism binder systems.

Nevertheless, many IOTs contain a high proportion of crystalline phases and a relatively low amorphous fraction, which can inherently limit precursor reactivity (Han et al., 2017; Zhang N. et al., 2021). This constraint can be substantially mitigated through activation strategies. Mechanical activation (e.g., grinding) reduces particle size and increases specific surface area, expanding reactive sites via lattice distortion and defect generation (Yao et al., 2020; Saedi et al., 2020; Patra et al., 2019). Thermal treatments enhance reactivity through dehydroxylation of clay minerals and partial amorphization of crystalline silicates, while chemical activation (e.g., NaOH fusion; acid leaching followed by reprecipitation) enables the production of highly reactive sodium silicate powders directly from IOT (Li C. et al., 2009; Starostina, 2018; Figueiredo et al., 2021; Hu et al., 2024). These treatments increase amorphous content, partially cleave Si–O–Si and Al–O–Si bonds, and generate new reactive surfaces, transforming IOT into both an active precursor and a reactive filler that improves particle packing (Saedi et al., 2020; Yao et al., 2020; Wei et al., 2023).

The performance of IOT in geopolymer and alkali-activated systems has been widely validated experimentally. Appropriate replacement levels in fly ash–based geopolymer pastes improve fresh properties, compressive strength, and high-temperature microstructural stability (Duan et al., 2016a). Fly ash–IOT porous geopolymers have proven suitable for adsorption (e.g., Cu(II) removal) and lightweight construction (Duan et al., 2016b). Reuse of IOT as fine aggregate in geopolymer mortars achieves high compressive strength and acceptable workability with optimized grading and binder-to-waste ratios (Hu et al., 2019; Defáveri et al., 2019). High IOT contents in fly ash–slag geopolymer bricks also yield favorable strength and microstructural development, particularly under combined alkali activation (Kumar et al., 2017; Bezerra et al., 2019). Moreover, sodium silicate powders derived from IOT can function as activators in one-part geopolymer binders, demonstrating direct integration of tailings-derived silica into geopolymer chemistry (Figueiredo et al., 2021).

Using IOT as aggregate further provides advantages: rough, angular particles enhance mechanical interlocking at the aggregate–paste interface and strengthen the ITZ, which is especially beneficial for ultra-high-performance geopolymer concrete (UHPGPC), enabling high strength and low permeability (Zhao et al., 2021; Huang et al., 2024). IOT's oxide composition and partial amorphous content promote co-formation of N–A–S–H, C–(A)–S–H, and M–(A)–S–H gels, increasing matrix density. IOT has also served as a reactive silica source for mesoporous silica and ceramsite-type lightweight aggregates (Lu et al., 2020; Sun et al., 2021; Wang Y.-S. et al., 2020). Thus, IOT functions not as an inert filler but as an active component enhancing reactivity, microstructural continuity, and mechanical performance (Zhang N. et al., 2021; Defáveri et al., 2019; Wei et al., 2023).

Finally, IOT utilization in geopolymer systems offers environmental risk mitigation via chemical and physical immobilization of heavy metals within the three-dimensional geopolymer network, providing a safe and value-added pathway for IOT and compositionally similar wastes (Zhan et al., 2018, 2022; Liu et al., 2023; Wang Y. et al., 2023). In this manner, IOT transitions from a high-volume, environmentally burdensome waste into a strategic raw material for low-carbon, durable, and resource-efficient geopolymer binders (Osinubi et al., 2015; Yellishetty et al., 2008; Lebre et al., 2017).

REFERANCES

Adiansyah, J. S., Rosano, M., Vink, S., & Keir, G. (2015). A framework for a sustainable approach to mine tailings management: Disposal strategies and re-use options. Journal of Cleaner Production, 108, 1050–1062.

Adiguzel, O., Kizilkanat, A. B., & Gencel, O. (2022). A comprehensive review on the use of mining tailings as a sustainable construction material. Construction and Building Materials, 340, 127784.

Almeida, D. R., Silva, T. H., & Costa, L. M. (2021). Iron ore tailings as precursors for alkali-activated materials: Mineralogical and chemical aspects. Journal of Materials Research and Technology, 14, 2300–2312.

Almeida, D. R., Zhang, J., & Costa, L. M. (2023). Current status and utilization potential of iron ore tailings in China. Resources, Conservation and Recycling, 192, 106954.

Armstrong, M., Petter, R., & Petter, C. (2019). Why have so many tailings dams failed in recent years? Resources Policy, 63, 101412.

Andini, S., Cioffi, R., Colangelo, F., Grieco, T., Montagnaro, F., & Santoro, L. (2008). Coal fly ash as raw material for the manufacture of geopolymer-based products. Waste Management, 28(2), 416–423.

Brown, K., & Milke, M. (2016). Recycling mine tailings in chemically bonded ceramics—A review. Journal of Environmental Management, 184, 353–364.

Carvalho, J. M. F., Defáveri, K., Mendes, J. C., Schmidt, W., & Kühne, H. C. (2021). Influence of particle size-designed recycled mineral admixtures on the properties of cement-based composites. Construction and Building Materials, 272, 121640.

Castro-Gomes, J. P., Silva, A. P., Cano, R. P., Suarez, J. D., & Albuquerque, A. (2012). Potential for reuse of tungsten mining waste-rock. Journal of Cleaner Production, 25, 34–41.

Chandran, G., Ashish, S., Ajayan, A. S., & Selvaraj, T. (2026). Selection criteria for mine tailings as SCM: A comprehensive review of types, properties and performance. Minerals Engineering, 235, 109822.

Cui, X., et al. (2019). Environmental impact of the Canela tailings dam failure in Mexico. Environmental Science and Pollution Research, 26, 24567–24580.

Cui, X., Geng, Y., Li, T., Zhao, R., Li, X., & Cui, Z. (2021). Field application and effect evaluation of different iron tailings soil utilization technologies. Resources, Conservation and Recycling, 173, 105746.

da Silva, R., Ramos, L. T., & Oliveira, P. T. (2022). Environmental implications of iron tailings storage and reuse. Resources, Conservation and Recycling, 185, 106473.

Davila, R. B., Fontes, M. P. F., Pacheco, A. A., & Ferreira, M. S. (2020). Heavy metals in iron ore tailings and floodplain soils affected by the Samarco dam collapse. Science of the Total Environment, 709, 136151.

Davidovits, J. (1991). Geopolymers: Inorganic polymeric new materials. Journal of Thermal Analysis, 37(8), 1633–1656. https://doi.org/10.1007/BF01912193

Defáveri, K., Santos, L., Carvalho, J., et al. (2019). Iron ore tailing-based geopolymer containing glass wool residue: A study of mechanical and microstructural properties. Construction and Building Materials, 220, 375–385.

Du, J., Meng, W. N., Hayat, K. H., et al. (2021). New development of ultra-high-performance concrete (UHPC). Composites Part B: Engineering, 224, 109220.

Duxson, P., Fernández-Jiménez, A., Provis, J. L., Lukey, G. C., Palomo, A., & van Deventer, J. S. J. (2007). Geopolymer technology: The current state of the art. Journal of Materials Science, 42, 2917–2933.

De Azevedo, A. R. G., Marvila, M. T., Gomes, T. N., & Cecílio, M. V. T. (2021). Influence of agro-industrial wastes on the physical and mechanical performance of geopolymer mortars. Journal of Cleaner Production, 289, 125136.

Deb, P. S., Nath, P., & Sarker, P. K. (2014). The effect of ground granulated blast-furnace slag blending with fly ash and activator content on the workability and strength properties of geopolymer concrete. Materials & Design, 62, 32–39.

Duan, P., Yan, C., Zhou, W., & Ren, D. (2016a). Fresh properties, compressive strength and microstructure of fly ash geopolymer paste blended with iron ore tailing under thermal cycle. Construction and Building Materials, 118, 76–88.

Duan, P., Yan, C., Zhou, W., & Ren, D. (2016b). Development of fly ash and iron ore tailing based porous geopolymer for removal of Cu(II) from wastewater. Ceramics International, 42(13), 13507–13518.

Ferreira, I. C., Galery, R., Henriques, A. B., Teixeira, A. P. D., Prates, C. D., Lima, A. S., & Souza, I. R. (2022). Reuse of iron ore tailings for production of metakaolin-based geopolymers. Journal of Materials Research and Technology, 18, 4194–4200.

Figueiredo, R. A. M., Brandão, P. R. G., Soutsos, M., Henriques, A. B., & Mazzinghy, D. B. (2021). Producing sodium silicate powder from iron ore tailings for use as an activator in one-part geopolymer binders. Materials Letters, 288, 129333.

Gollakota, A. R. K., Volli, V., & Shu, C. M. (2019). Progressive utilisation prospects of coal fly ash: A review. Science of the Total Environment, 672, 951–989.

Hamada, H. M., Al-Attar, A., Askar, M. K., Beddu, S., & Majdi, A. (2025). Enhancing sustainable concrete with iron ore tailings as fine aggregate: Environmental and engineering perspectives. Construction and Building Materials, 470, 140707. https://doi.org/10.1016/j.conbuildmat.2024.140707.

Han, J., Wang, S., & Zhang, Y. (2017). Characteristics and reuse potential of iron ore tailings in China. Minerals, 7(11), 200.

Hu, Z., Gu, X., Cheng, B., Wang, Q., Liu, J., Ge, X., Yin, S., 2024. The Role of Chemical Activation in Strengthening Iron Ore Tailings Supplementary Cementitious Materials. Buildings 2024, Vol. 14, Page 963 14, 963. DOI: 10.3390/ BUILDINGS14040963.

Huang, X., Tian, Y., Jiang, J., Lu, X., He, Z., & Jia, K. (2024). Mechanical properties and enhancement mechanism of iron ore tailings as aggregate for manufacturing ultra-high performance geopolymer concrete. Construction and Building Materials, 439, 137362.

Jiang, L., Chen, X., & Wang, H. (2022). Statistical analysis of iron ore tailings production and utilization in China. Journal of Cleaner Production, 357, 131921.

Kaze, R. C., Beleuk, A., Moungam, L. M., Fonkwe Djouka, M. L., Nana, A., & Kamseu, E. (2017). The corrosion of kaolinite by iron minerals and the effects on geopolymerization. Applied Clay Science, 138, 48–62.

Kossoff, D., Dubbin, W. E., Alfredsson, M., Edwards, S. J., Macklin, M. G., & Hudson-Edwards, K. A. (2014). Mine tailings dams: Characteristics, failure, environmental impacts, and remediation. Applied Geochemistry, 51, 229–245.

Kumar, R., Das, P., Beulah, M., Arjun, H. R. R., & Ignatius, G. (2017). Utilization of iron ore tailings for the production of fly ash–GGBS-based geopolymer bricks. Journal of Advanced Manufacturing Systems, 16(4), 275–290.

Kuranchie, F., Yellishetty, M., & Mostafa, A. (2015). Reuse of iron ore tailings from Western Australia. Journal of Sustainable Mining, 14(4), 173–181.

Kuranchie, F. A., Shukla, S. K., & Habibi, D. (2016). Utilisation of iron ore mine tailings for the production of geopolymer bricks. International Journal of Mining, Reclamation and Environment, 30(2), 92–114.

Lebre, É., Corder, G., & Golev, A. (2017). The role of the mining industry in a circular economy: A framework for resource management at the mine site level. Journal of Industrial Ecology, 21(3), 662–672.

Li, Y., Li, S., Pan, X., Zhao, X., & Guo, P. (2023). Eco-friendly strategy for preparation of high-purity silica from high-silica iron ore tailings using S-

HGMS coupling with ultrasound-assisted fluorine-free acid leaching technology. Journal of Environmental Management, 339, 117932.

Li, C., Sun, H., Wei, X., & Li, L. (2009). Iron ore tailings used for the preparation of cementitious material by compound thermal activation. International Journal of Mineral, Metallurgy and Materials, 16(4), 355–358.

Liu, X. Y., Xie, X., Liu, R. D., Lyu, K., Wang, X. Y., Yu, J. Y., Fu, F., Wu, C. Y., & Zuo, J. Q. (2023). Manufacture of alkali-activated cementitious materials using municipal solid waste incineration fly ash (MSWI FA): The effect of the Si/Al molar ratio on fresh and hardened properties. Construction and Building Materials, 409, 134075.

Lu, C., Yang, H., Wang, J., Tan, Q., & Fu, L. (2020). Utilization of iron tailings to prepare high-surface-area mesoporous silica materials. Science of the Total Environment, 736, 139483.

Luukkonen, T., Abdollahnejad, Z., Yliniemi, J., Kinnunen, P., & Illikainen, M. (2018). One-part alkali-activated materials: A review. Cement and Concrete Research, 103, 21–34.

Makarov, D. V., Konina, O. T., & Goryachev, A. A. (2021). Dusting suppression at tailings storage facilities. Journal of Mining Science, 57(4), 681–688.

Marvila, M. T., Azevedo, A. R. G., Oliveira, L. M., Pereira, F. T., & Alexandre, J. (2021). Use of glass polishing waste in geopolymer binder production. Construction and Building Materials, 284, 122748.

Nematollahi, B., & Sanjayan, J. (2014). Effect of activator combinations on fly ash geopolymer. Materials & Design, 57, 667–672.

Osinubi, K. J., Yohanna, P., & Eberemu, A. O. (2015). Cement modification with iron ore tailings. Transportation Geotechnics, 5, 35–49.

Panda, B., Singh, G. B., Unluer, C., & Tan, M. J. (2019). Synthesis and characterization of one-part geopolymers for extrusion-based 3D concrete printing. Journal of Cleaner Production, 220, 610–619.

Patra, S., Pattanaik, A., Venkatesh, A. S., & Venugopal, R. (2019). Mineralogical and chemical characterization of low grade iron ore fines from Barsua area, Eastern India with implications on beneficiation and waste utilization. Journal of the Geological Society of India, 93, 443–454.

Provis, J. L., & van Deventer, J. S. J. (2014). Alkali activated materials: State-of-the-art report. RILEM TC 224-AAM.

Ramos, L. T. da Silva, Lima, K. A., de Oliveira, P. T., & Lima, R. K. (2024). Iron ore tailings as a new product: A review-based analysis of its potential incorporation capacity by the construction sector. Cleaner Waste Systems.

Saedi, A., Jamshidi-Zanjani, A., & Darban, A. K. (2020). A review on different methods of activating tailings to improve their cementitious property as cemented paste and reusability. Journal of Environmental Management, 270, 110881.

Saldanha, R. B., Caicedo, A. M. L., de Araújo, M. T., Scheuermann Filho, H. C., Moncaleano, C. J., Silva, J. P. S., & Consoli, N. C. (2023). Potential use of iron ore tailings for binder production: A life cycle assessment. Construction and Building Materials, 365, 130008.

Schoenberger, E. (2016). Environmentally sustainable mining: The case of waste tailings. Resources Policy, 49, 119–128.

Scrivener, K. L., John, V. M., & Gartner, E. M. (2018). Eco-efficient cements: Potential economically viable solutions for a low-CO2 cement-based materials industry. Cement and Concrete Research, 114, 2–26. https://doi.org/10.1016/j.cemconres.2018.03.015

Silva Rotta, L. H., Alcantara, E., Park, E., Negri, R. G., Lin, Y. N., Bernardo, N., et al. (2020). The 2019 Brumadinho tailings dam collapse: Possible cause and impacts of the worst human and environmental disaster in Brazil. International Journal of Applied Earth Observation and Geoinformation, 90, 102119.

Soltani, N., Keshavarzi, B., Moore, F., et al. (2021). In vitro bioaccessibility, phase partitioning, and health risk of potentially toxic elements in dust of an iron mining and industrial complex. Ecotoxicology and Environmental Safety, 212, 111972.

Starostina, I. V. (2018). The through-dyed autoclaved silicate concretes with the use of thermally activated iron ore raw materials refinement tailings. Solid State Phenomena, 284, 1101–1106.

Sun, Y., Zhang, X., Han, Y., & Li, Y. (2020). A new approach for recovering iron from flotation tailings via suspension magnetization roasting in a mixture of CO and H2 followed by magnetic separation. Powder Technology, 361, 571–580.

Sun, Y., Zhang, X., Han, Y., & Li, Y. (2021). Preparation of lightweight aggregates from iron ore tailings and coal fly ash. Construction and Building Materials, 270, 121406.

Tharwat, A., Li, J., Sun, X., & Şengör, S. S. (2023). Bioremediation and biocementation of mine tailings: A sustainable approach for environmental management. Environmental Technology & Innovation, 103606.

Thejas, H. K., & Hossiney, N. (2021). A short review on environmental impacts and application of iron ore tailings in sustainable eco-friendly bricks. Materials Today: Proceedings.

Wang, X. J., Chen, S., & Zhang, Z. (2023). Enhancing the pozzolanic activity of iron ore tailings by mechanical activation for alkali-activated materials. Cement and Concrete Composites, 139, 105040.

Wang, Y., Ma, J., Qing, L., Liu, L., Shen, B., Li, S., & Zhang, Z. (2023). Accelerated carbonation pretreatment of municipal solid waste incineration fly ash and its conversion to geopolymer with coal fly ash. Construction and Building Materials, 383, 131363.

Wang, Y.-S., Alrefaei, Y., & Dai, J.-G. (2020). Influence of coal fly ash on the early performance enhancement and formation mechanisms of silico-aluminophosphate geopolymer. Cement and Concrete Research, 127, 105932.

Wei, M. L., Wei, W., Li, Y., et al. (2023). Maximizing the pozzolanic potential of superfine iron tailings for low-carbon stabilization: Application of high-calcium geopolymer. Resources, Conservation & Recycling, 198, 107198.

Yao, G., Wang, Q., Su, Y., Wang, J., & Lyu, X. (2020). Mechanical activation as an innovative approach for the preparation of pozzolan from iron ore tailings. Minerals Engineering, 145, 106068.

Yellishetty, M., Karpe, V., Reddy, E. H., Subhash, K. N., & Ranjith, P. G. (2008). Reuse of iron ore mineral wastes in civil engineering constructions: A case study. Resources, Conservation and Recycling, 52(11), 1283–1289.

Zhan, X. Y., Wang, L. A., Hu, C. C., Gong, J., Xu, T. T., Li, J. X., Yang, L., Bai, J. S., & Zhong, S. (2018). Co-disposal of MSWI fly ash and electrolytic manganese residue based on geopolymeric system. Waste Management, 82, 62–70.

Zhan, X. Y., Wang, L. A., Gong, J., Deng, R., & Wu, M. (2022). Co-stabilization/solidification of heavy metals in municipal solid waste incineration fly ash and electrolytic manganese residue based on self-bonding characteristics. Chemosphere, 307, 135793.

Zhang, Z., Zhang, Z., Yin, S., & Yu, L. (2016). Utilization of iron tailings sand as environmentally friendly fine aggregate in high-strength concrete. Materials, 13(24), 5614.

Zhang, N., Tang, B., & Liu, X. (2021). Cementitious activity of iron ore tailing and its utilization in cementitious materials, bricks and concrete. Construction and Building Materials, 288, 123022.

Zhao, J., Ni, K., Su, Y., & Shi, Y. (2021). An evaluation of iron ore tailings characteristics and iron ore tailings concrete properties. Construction and Building Materials, 286, 122968.

Zhao, S., Zheng, K., Liao, D., Peng, L., Ni, L., Zhang, L., & Weng, R. (2026). Activation of iron tailings with a composite activator of NaOH and $CaSO_4 \cdot 2H_2O$ and its effect on the strength of iron tailings-based mortar specimens. Powder Technology, 467, 121564.

CHAPTER 3

The Necessary Analyses to Determine the Refractory Properties of Local Clays

Halil Eren[1]

[1] Lecturer Dr., Cankiri Karatekin University, Materials and Materials Processing Technologies Department, ORCID: 0000-0002-4224-683X

Introduction

Clay minerals have been used for many purposes since prehistoric times. Products like bricks, pottery, and simple household items were made from clay minerals in prehistoric times (Injor et al., 2025). Along with the development of industry, the iron and steel sector in particular has also developed. The importance of using refractory materials in the construction of furnaces and ovens in the industrial field has increased (Injor et al., 2025). In this context, the evaluation of local clays for refractory production is becoming quite important from a cost perspective. The use of local resources helps reduce dependence on imports and costs while increasing production (Injor et al., 2025). The manufacturing of furnaces in the metallurgy sector and coatings in the cement and ceramics sectors is quite expensive. Therefore, evaluating local clays to investigate and develop their refractory properties is of industrial importance (Mokwa et al., 2019). Additionally, with appropriate enrichment methods, these clays can be developed for use in the petrochemical industry. They are also used in energy facilities with high thermal resistance due to their high heat resistance (Mokwa et al., 2019).

Properties of Clays

Clay is generally a mineral that can be shaped with enough water and solidifies when dried or fired (Ameh & Obasi, 2009). Although clays are generally composed of silicate layers, it also contains other minerals (Irabor, 2002). Clays can exhibit different characteristics depending on their location (Injor et al., 2025). Clay materials lose their chemically bound water and fluidity at approximately 500 °C, becoming harder. Between 950-1350 °C, its strength increases (Mazen, 2009). Table 1 shows the composition of a refractory clay according to international standards (Mazen, 2009).

Table 1. Chemical composition of refractory clays according to international standards.

Constituent	Fired Clay (%)	Refractory bricks (%)
SiO_2	55 – 75	51 – 70
Al_2O_3	25 – 45	25 – 40
Fe_2O_3	0.5 – 2.0	0.5 – 2.4
K_2O	< 2.0	
MgO	< 2.0	
LiO	12.15	

The refractoriness properties of the kiln can be determined based on its resistance to high temperatures, heat flow, volume stability at high temperatures, thermal shock resistance, corrosion, and wear (Injor et al., 2025). Upon

examining Table 1, it is evident that the majority of the refractory clay, classified as firebrick or kaolin, is kaolinite (Al_2O_3. $2SiO_2$. $2H_2O$) minerals are formed. Kaolin-based clays and fire clays do not have an alumina-silica ratio of 1:2, contain more than 30% alumina, and have a Sulphur (Fe_2SO_3) content of less than 2.0% (Injor et al., 2025).

Refractory Materials

Refractory materials are heat-resistant materials that show resistance to thermal shock and chemical attacks. Therefore, they are used in the inner linings of furnaces. They are also used in products such as rockets, flame detector systems, crucibles, etc. (Yami & Umaru, 2007). During operation, it retains heat within the system to ensure energy efficiency, and additionally protects structural and functional components from heat damage. In summary, refractory materials are highly important materials for protecting industrial equipment and ensuring the efficiency and safety of industrial processes at high temperatures (Yami & Umaru, 2007).

Refractory materials are divided into three groups based on their chemical behaviour: acidic, basic, and neutral (Yami & Umaru, 2007). Acidic refractory materials such as SiO_2 (Silica) and fireclay are resistant to corrosive substances like slag in these environments. However, materials known as basic refractories, such as MgO (Magnesite) and $CaMg(CO_3)_2$ (Dolomite), are more resistant in basic environments. Therefore, basic refractories are frequently used in the steel production industry. Materials such as Al_2O_3 (Alumina) and $FeCr_2O_4$ (Chromite), which are called neutral refractories, are preferred for use in many industrial fields because they are resistant to all environments (Rajput, 2015). For the selection of refractory material types and the appropriate determination of their application areas, it is crucial to well-define their thermal performance and properties (Rajput, 2015).

Properties of Refractory Materials

Refractory materials stand out for their high-temperature applications due to their specific properties and the necessary characteristics for such environments. The suitability of refractory materials in their application areas is related to a balanced combination of these properties.

1. Bulk Density

Bulk density is defined as the weight per unit volume of porous refractory materials. Bulk density is directly related to product quality, and materials with high bulk density also have high quality. For the calculation of bulk density, the clay is dried in an oven at a temperature of 110 ˚C for 24 hours. The dry weight of the sample (Wd) is determined. The material is then baked in the oven. The sample is then placed in a beaker of water and its wet weight (Ws) is recorded (ASTM, 2008). The sample extracted from the water is suspended and its

suspended weight (Wp) is determined. Bulk density (Bd) is calculated using the equation shown in equation 1 (ASTM, 2008).

$$Bd = \frac{Wd}{Ws-Wp} \quad (1)$$

2. Moisture Content

Water content is generally defined as the ratio of the water mass to the dry matter mass of the water body. Generally, it is shown as a percentage. The clay sample is weighed after being removed from the first mould and before drying. This is determined as the wet mass (Gw). After drying and cooling in the sample dryer, the sample is weighed again. This is also determined as dry mass (Gd). The moisture content of the sample is determined using the following equation (ASTM, 2008). MC also shows the content.

$$MC = \frac{Gw-Gd}{Gd} \text{x} 100\ \% \quad (2)$$

3. Firing Shrinkages

Firing shrinkage is an irreversible deformation phenomenon observed in refractory clays during drying and firing under specific conditions. The sample is first dried in an oven at 100 °C for 24 hours. After that, the temperature is increased in a controlled manner at specific intervals, heating it up to 1100 °C (ASTM, 2001). The cooking shrinkage of the sample is calculated using equation 3 shown below (ASTM, 2001). Here, ΔL represents the change in length, which is the difference between the final and initial lengths, while Lo represents the initial length.

$$FS = \frac{\Delta L}{Lo} \text{x} 100\ \% \quad (3)$$

4. Water Absorption

The water absorption property is a test method that indicates how much water the clay can absorb before it degrades (Yokoyama, 1985). The clay sample is first dried in an oven to remove any moisture. After drying, the dry weight of the sample is measured (Wd). Later, the sample is suspended in a container filled with hot water so that it does not touch the bottom. After the sample is boiled in water for 4 hours, it is cooled to room temperature (Yokoyama, 1985). For example, the sample is reweighed to determine its saturated weight (SW) (Yokoyama, 1985). Water absorption percentage (WA) is calculated using equation 4.

$$WA = \frac{SW-Wd}{Wd} \text{x} 100\ \% \quad (4)$$

5. Thermal Shock Resistance

Thermal shock resistance allows us to learn about a refractory material's ability to withstand sudden temperature changes based on its application in industrial furnaces or melting furnaces (Rajput, 2015). The clay test sample is prepared to the ideal size and placed in an oven heated to 900 °C. The sample is removed from the oven after being left inside for 10 minutes. After being allowed to cool for a certain period, the sample is then placed back in the furnace at 900 °C and kept there for 10 minutes. This process is continued until a crack form on the sample surface due to the sudden temperature change. The number of cycles at the moment the crack forms is recorded (Rajput, 2015).

6. Apparent Porosity

Porosity in refractory materials refers to the total volume of pores that can be filled with slag, fluids, vapors, molten metal, etc., causing serious damage to the refractory's structure (Olusola, 2014). Porosity in refractory materials is measured as the average percentage relative to the total volume. Sample 110 °C is dried evenly in an oven at 110 °C for 24 hours, and then fired at 1100 °C. First, the dry weights are determined. After that, they are cooled to room temperature by being immersed in water (Olusola, 2014). Apparent porosity (P) is calculated according to equation 5.

$$P = \frac{W-D}{W-S} \text{ x } 100 \qquad (5)$$

Here, the symbols W, D, and S represent the wet, dry, and suspended weights, respectively.

7. Refractoriness

To measure the refractoriness property, clay cones are obtained from the samples and dried. Cones are placed in the middle of a refractory plate. The sample is loaded into the furnace and a controlled temperature increase is performed at a rate of 10 C per minute. The heating process continues in the oven until the tip of the test cone bends. The refractory property can also be calculated using Shuen's formula in equation 6 (Agbo et al., 2022).

$$Refractoriness = \frac{360+Al2O3-Ro}{0.228} \qquad (6)$$

Here, Al_2O_3 represents alumina, and RO represents the oxides found in clay.

8. Refractoriness under load

Refractoriness Under Load (RUL) is a method used to determine the deformation of refractory materials after continuous application of a load at high temperatures (Aremu et al., 2013). A cylindrical test specimen of specific dimensions is subjected to a compressive force. After that, it is cooked to a

predetermined temperature. The data obtained determines the refractory properties under load (Aremu et al., 2013).

9. Cold Crushing Strength

Cold crushing strength or compressive strength (CSS) is the process of applying a load to a test specimen placed on a flat platform using a press. Loading continues until refractory cracks form. The highest stress obtained after cracking occurs gives the sample's CSS. The cold crushing strength is shown in equation 7 (Injor et al., 2025).

$$CSS = \frac{Lenght}{Area} \quad (7)$$

10. Grain Size Analysis

Grain size analysis measures the diameters of sediments (Injor et al., 2025). Standard sieves are used. The clay is weighed before processing and passed through sieves on a mechanical shaker. It is shaken for the specified duration, and then the mass on each sieve is calculated. The percentage passing and the percentage retained (PR) for each sieve are determined as shown in equation 8 (Injor et al., 2025).

$$PR = \frac{WR}{WI} \text{ x } 100 \quad (8)$$

Here, WI represents the initial weight, while WR represents the protected weight.

11. Thermal Expansion

When refractory materials are heated, changes occur in their size and density. To determine the thermal expansion coefficient of a refractory material, the sample is fixed to the base of a calorimeter. The specimen length (L) is determined by measuring from the inner edge of the specimen to the other edge. As the temperature changes (ΔT), there is also a change in length (ΔL) (Olalere et al., 2019). The thermal expansion formula is shown in equation 9. Here, α represents the coefficient of thermal expansion (Olalere et al., 2019).

$$\alpha = \frac{\Delta L}{Lx\Delta T} \text{ x } 100 \quad (9)$$

Result

Clays has been used in many fields throughout human history. Its importance has increased with the development of industrialization in refractory construction. Determining the refractory properties of local clays and incorporating them into industry is extremely important for many reasons, including cost, industrialization, reducing external dependence, and more. Refractoriness properties can be determined and evaluated for use through specific experiments applied to local clays.

References

Agbo, A. O., Nwogbu, C. C., & Udeh, B. C. (2022). Engineering Characterization of Agbani Clay Deposit as Refractory Material for Furnace Lining.

Ameh, E. M., & Obasi, N. L. (2009). Effect of rice husk on insulating bricks produced with Nafuta and Nsu clays. *Global Journal of Engineering and Technology*, *2*(4), 661-668.

American Society for Testing and Materials, (2008). *ASTM C71-08: Standard Terminology Relating to Refractories,* vol. 15.1.

Aremu, D. A., Aremu, J. O., & Ibrahim, U. H. (2013). Analysis of Mubi clay deposit as a furnace lining. *Int. J. Sci. Technol. Res*, *2*, 182-186.

ASTM C326-01, (2001). Standard Methods for Drying and Fired Shrinkages of Ceramic Whiteware Clays. *West Conshohocken, PA: ASTM International,* vol. 15.2.

Injor, O. M., Sadiku, E. R., Teffo, M. L., Ramakokovhu, M. M., Agbogo, V. U., & Kupolati, W. K. (2025). Advances in the Development, Processing, and Application of Locally Sourced Clay-based Refractory Materials for Furnace Application in Nigeria. *Science, Engineering and Technology*, *5*(2), 193-208.

Irabor, P. S. A. (2002). Physical and chemical investigation on some Nigerian kaolinite clays for use in the ceramics and allied industries. *Nigerian journal of engineering research and development*, *1*(1), 54-59.

Mazen, N. A. (2009). Production of fire clay refractory bricks from local materials. *European journal of scientific Research*, *26*(3), 386-392.

Mokwa, J. B., Lawal, S. A., Abolarin, M. S., & Bala, K. C. (2019). Characterization and evaluation of selected kaolin clay deposits in Nigeria for furnace lining application. *Nigerian Journal of Technology*, *38*(4), 936-946.

Olalere, A. A., Yaru, S. S., & Dahunsi, O. A. (2019). Evaluation of the chemical and thermo-physical properties of locally aggregated kaolin-based refractory materials. *Journal of Mechanical Engineering and Sciences*, *13*(1), 4743-4755.

Olusola, E. O. (2014). Characterization of local bentonite clays for application in the foundry industry. *Unpublished PhD project, Department of Mechanical Engineering, Federal University of Technology Minna*, 10-15.

Rajput, R. K. (2015). *Engineering materials 3rd ed*. S. Chand Publishing.

Yami, A. M., & Umaru, S. (2007). Characterization of some Nigerian clays as refractory materials for furnace lining. *Continental Journal of Engineering Sciences*, *2*, 30-35.

Yokoyama, S. (1985). Measurement of Apparent Porosity, Water Absorption and Densities of Refractory Bricks. *J. CERAM. SOC. JAP. J. Ceram. Soc. Jap.*, *93*(10), 655.